Chapter 1

Introduction

Quantum Chromodynamics (QCD) is widely accepted as a fundamental theory which describes the strong interactions because of its remarkable success in the high precision tests of the high energy experiments. Although we believe QCD is the fundamental theory, it is difficult to study a scattering process with a small momentum transfer in the framework of the QCD since the renormalized coupling constant is not small enough in such a low energy scale to use a perturbative technique.

The single diffractive dissociation [1] (or single diffraction) is one of such processes that we cannot fully describe in the framework of QCD. The single diffraction is experimentally defined as a process where one of the two oppositely incoming hadrons keeps its quantum numbers unchanged after the collision. This leading hadron usually go off in the beam pipe without decreasing its initial momentum. In the view point of the quantum field theory, any process should be explained by the exchange of field(s) between the two hadrons. The exchanged field(s) in the single diffraction should not carry a color in total so as to keep the hadrons as a color singlet. This exchanged color-less object is a *pomeron* named in the old *Regge pole phenomenology* [2, 3].

The Regge pole phenomenology is based on the observed hadron spectroscopy and some general postulates such as the unitarity and the analytic-

ity of the S-matrix. The validity of the Regge pole phenomenology is limited in the soft (small momentum transfer) process. In the Regge picture, a scattering process is described as an exchange of "pole", which lives in the complex angular momentum space. The pomeron is introduced as one of such poles which give a dominant contribution to soft collisions of hadrons with high energy. At least in the soft process, pomeron behaves as if it is a virtual particle state although it has not been observed in the hadron spectroscopy. The Regge pole phenomenology is briefly described in Appendix A.

The uniqueness of the *hard* single diffraction is an existence of the two different scales in a single interaction. Regarding to the leading hadron, a momentum transfer via the pomeron is too small to use the perturbative QCD but it is small enough to use the Regge pole picture. On the other hand, the interaction between the constitutions of the pomeron and the dissociating hadron take place in a hard scale where we could use the perturbative QCD. It is thus possible to probe the "contents" of the pomeron by studying the hard single diffraction using a combination of the Regge phenomenology and the perturbative QCD. The pomeron is treated as an effective particle state in the above picture called Ingelman-Schlein model (IS model) [4].

Experimental study of the partonic nature of the pomeron was pioneered by UA8 experiments [5, 6] by observing dijet production in the single diffraction events at CERN $Sp\bar{p}S$ collider operated at $\sqrt{s}$=630 GeV. They reported that the pomeron exhibits a "hard structure" like $zf(z) \sim 1 - z$ basically, where z is a parton momentum fraction in the pomeron. More recently, both ZEUS and H1 collaboration measured the structure function of the pomeron by the deep inelastic scattering experiment at the HERA e-p collider. The measured pomeron structure function is mostly "flat" like $zf_{q,g/I\!P}(z) \sim 1$ and depends on Q^2 slightly. The H1 [7] performed a NLO QCD fit for the observed pomeron structure function at different Q^2 scales

and concluded approximately 90%(80%) of the momentum is carried by gluons at Q^2=4.5GeV^2(75 GeV^2) under such model. The ZEUS [8] measured both the pomeron structure function and the differential cross section of the diffractive dijet photoproduction. They also reported that a substantial part of the pomeron momentum is carried by gluons if the pomeron is assumed to have a hadron-like partonic structure in the form of parton densities which evolve according to the DGLAP equations [9].

At the Tevatron collider, the dijet production [10] and the W-boson production [11] were observed in the diffractive $p\bar{p}$ scattering at $\sqrt{s}$=1800 GeV. The combined analysis of the diffractive dijet and the diffractive W productions support a dominantly gluonic picture of the pomeron. The measured rates of these processes show significantly lower values than the IS model prediction with the Donnachie-Landshoff flux (see Sec. 1.2). This result suggest that there is a problem in the hypothesis of the factorization of the pomeron flux at the Tevatron energy although the hypothesis successfully described the data at the HERA [42].

The study of the diffractive heavy flavor production can also allow us to test the IS model [12]. The diffractive heavy flavor production rate is sensitive to the contribution of the gluon in the pomeron because the heavy flavors are mainly produced through a gluon-gluon fusion. The experimental study of the diffractive heavy flavor production was first reported by the UA1 collaboration at CERN $Sp\bar{p}S$ collider [13]. They searched for the diffractively produced μ+jet events and estimated the heavy flavor contribution in the data by subtracting non-heavy flavor backgrounds. Assuming the hard structure function to the pomeron they found an upper limit of the diffractive $b\bar{b}$ production cross section $\sigma_{b\bar{b}}(p_T > 8\text{GeV})$<50 nb (95% C.L.) at $\sqrt{s}$=630 GeV.

In this thesis we present the first observation of the diffractive bottom

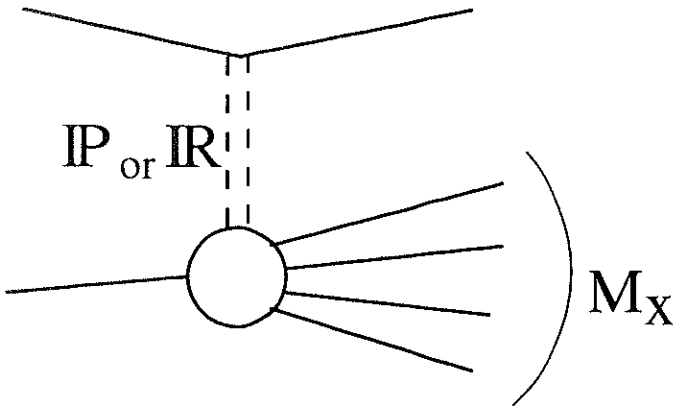

Figure 1.1: Single diffraction.

quark (b-quark) production in $p\bar{p}$ collisions at $\sqrt{s}$=1.8 TeV using the Collider Detector at Fermilab (CDF). The production of the b-quark is identified with both the large transverse momentum of the decaying electron relative to the associating jet axis and the large impact parameter of the electron track. The ratio of the diffractive b-quark production to the non-diffractive b-quark production is measured. The ratio is compared to the theoretical prediction of the Ingelman-Schlein model using the Donnachie-Landshoff flux.

1.1 Kinematics of the single diffraction

The single diffraction dissociation process, $p + \bar{p} \to p + X$ is schematically shown in Fig. 1.1. Some kinematical variables are frequently used to describe the single diffraction process. Using the four momentum of the initial beam particles ($P^{p\text{in}}, P^{\bar{p}\text{in}}$) and the final systems, ($P^{p\text{out}}, P^{X}$), the following three independent variables are defined;

$$s \equiv (P^{p\text{in}} + P^{\bar{p}\text{in}})^2 = (P^{p\text{out}} + P^{X})^2 \tag{1.1}$$

$$t \equiv (P^{p\text{out}} - P^{p\text{in}})^2 = (P^{X} - P^{\bar{p}\text{in}})^2 \tag{1.2}$$

$$M_X \equiv (P^{X})^2 = (P^{p\text{in}} + P^{\bar{p}\text{in}} - P^{p\text{out}})^2 \tag{1.3}$$

where s is a center of mass energy, t is a momentum transfer and M_X is a mass of diffractive system X. Equation 1.2 can be expressed by the energy of the system X (E_X),

$$\begin{aligned} s &= (P^{p\text{out}} + P^X)^2 \\ &= P^X \cdot (P^{p\text{out}} + P^X) + P^{p\text{out}} \cdot (P^{p\text{out}} + P^X) \\ &= E_X\sqrt{s} + \frac{1}{2}(s - {M_X}^2 + {m_p}^2), \end{aligned}$$

where m_p is the mass of the proton. This formulae yields the following expression for the energy of the system X,

$$E_X = \frac{s + {M_X}^2 - {m_p}^2}{2\sqrt{s}}. \tag{1.4}$$

The 3-momentum of the leading proton $\vec{P}^{p\text{out}}$ can be expressed with s and M_X using Eq. 1.4,

$$\begin{aligned} \left|\vec{P}^{p\text{out}}\right|^2 &= \left|\vec{P}^X\right|^2 \\ &= {E_X}^2 - {M_X}^2 \\ &= \frac{[s - (m_p + M_X)^2][s - (m_p - M_X)^2]}{4s} \\ &\xrightarrow{s, M_X \gg m_p} \frac{(s - {M_X}^2)^2}{4s} \\ \therefore \left|\vec{P}^{p\text{out}}\right| &\approx \frac{s - {M_X}^2}{2\sqrt{s}} \end{aligned} \tag{1.5}$$

Now we introduce the another frequently used variable, the Feynman variable x_F,

$$x_F = \frac{P_z^{p\text{out}}}{P_z^{p\text{in}}}. \tag{1.6}$$

Since $P_z^{p\text{out}} \approx \left|\vec{P}^{p\text{out}}\right|$, we arrive at,

$$x_F \approx \frac{\left|\vec{P}^{p\text{out}}\right|}{P_z^{p\text{in}}} = \frac{2\left|\vec{P}^{p\text{out}}\right|}{\sqrt{s}} \approx 1 - \frac{{M_X}^2}{s}. \tag{1.7}$$

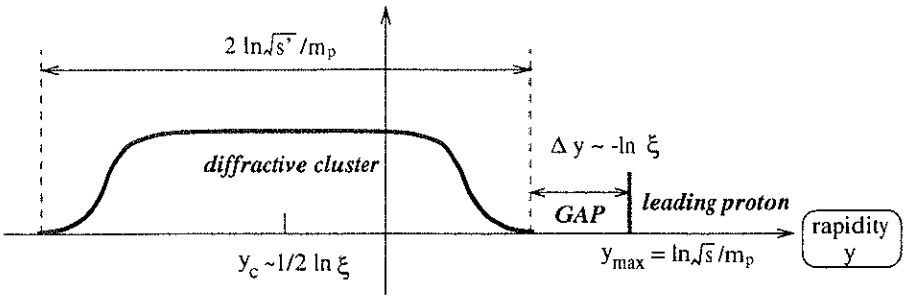

Figure 1.2: The kinematics of the single diffraction.

Instead of the x_F, the ξ variable is also used frequently,

$$\xi = \frac{{M_X}^2}{s} = 1 - x_F. \tag{1.8}$$

The rapidity distribution of the final states is schematically shown in Fig. 1.2. In the general $p\bar{p}$ collisions, the maximum rapidity bound of the generated particle is calculated from the definition,

$$\begin{aligned} y_{max} &= \frac{1}{2}\ln\frac{E+p_Z}{E-p_Z}\Big|_{max} = \frac{1}{2}\ln\frac{(E+p_Z)^2}{E^2-{p_Z}^2}\Big|_{max} \\ &\approx \frac{1}{2}\ln\frac{(2E_{beam})^2}{{m_p}^2} = \ln\frac{\sqrt{s}}{m_p} \end{aligned} \tag{1.9}$$

Thus the rapidity of the leading proton is $\ln\sqrt{s}/m_p$. The width of the diffractive system X can be calculated by using Eq. 1.9 at the center of mass frame of the system X,

$$y^X_{width} \approx 2\ln\frac{\sqrt{s'}}{m_\pi} = 2\ln\frac{M_X}{m_\pi} \tag{1.10}$$

The center of the rapidity for the diffractive system X is similarly obtained using Eqs. 1.4 and 1.5,

$$\begin{aligned} y^X_c &\approx -\frac{1}{2}\ln\frac{(E_X+|\vec{P}^X|)^2}{{M_X}^2} \approx -\frac{1}{2}\ln\frac{s^2}{s{M_X}^2} \\ &= -\frac{1}{2}\ln\frac{1}{\xi} \end{aligned} \tag{1.11}$$

Thus, the size of the rapidity gap between the cluster and the leading proton is obtained using Eq. 1.8,

$$\begin{aligned}\Delta y &= y^p_{max} - y^X_c - \frac{1}{2}y^X_{width} \\ &\approx \ln\frac{\sqrt{s}}{m_p} + \frac{1}{2}\ln\frac{1}{\xi} - \ln\frac{M_X}{m_\pi} \\ &= \ln\left(\frac{\sqrt{s}}{M_X}\frac{1}{\sqrt{\xi}}\frac{m_p}{m_\pi}\right) \\ &= -\ln\left(\xi\frac{m_\pi}{m_p}\right). \end{aligned} \tag{1.12}$$

The signature of the single diffraction is characterized with this forward rapidity gap.

1.2 Single diffraction in the Regge pole picture

A detailed analysis of the Regge pole phenomenology shows that the total cross section and the differential elastic cross section can be *factorized* into the Pomeron-hadron couplings and the universal contribution from the Pomeron exchange,

$$\sigma_T^{p\bar{p}} = \beta_{I\!P}^{pp}(0)\beta_{I\!P}^{\bar{p}\bar{p}}(0)\left(\frac{s}{s_0}\right)^{[\alpha_{I\!P}(0)-1]} \tag{1.13}$$

$$\frac{d\sigma_{el}^{p\bar{p}}}{dt} = \frac{1}{16\pi}[\beta_{I\!P}^{pp}(t)\beta_{I\!P}^{\bar{p}\bar{p}}(t)]^2\left(\frac{s}{s_0}\right)^{2[\alpha_{I\!P}(t)-1]} \tag{1.14}$$

where $\beta_{I\!P}^{pp}(\beta_{I\!P}^{\bar{p}\bar{p}})$ is a coupling of the pomeron to the proton(anti-proton) and the s_0 is a scale parameter introduced for dimensional convenience. The single diffraction dissociation can also be described in the framework of the Regge pole phenomenology using the triple Regge diagram. In the particular range of the kinematical region ($\xi \equiv M^2/s$ <0.1 [1]), the contribution from the pomeron exchange is dominant.

$$\frac{d\sigma_{sd}^{p\bar{p}}}{dt\,d\xi} = \frac{1}{16\pi}\beta_{I\!P}^{pp}(t)^2\xi^{1-2\alpha_{I\!P}(t)}\left[\beta_{I\!P}^{\bar{p}\bar{p}}(0)g(t)\left(\frac{s'}{s_0'}\right)^{\alpha_{I\!P}(0)-1}\right] \tag{1.15}$$

where $g(t)$ is a triple-pomeron coupling, $s' \equiv M^2$ is the square of the mass of the dissociating system, ξ is the fractional momentum of the pomeron carrying to the proton and s'_0 is the energy scale parameter. The triple-pomeron coupling $g(t)$ is experimentally found not to depend on t [1], thus $g(t) = g(0)$. The term in the brackets in Eq.1.15 can be identified as the pomeron-proton total cross section $\sigma_T^{p\mathbb{P}}$ in analogy with Eq.1.14. Then Eq.1.15 is expressed as,

$$\frac{d\sigma_{sd}^{p\bar{p}}}{dt\, d\xi} = f_{\mathbb{P}/p}(\xi, t)\sigma_T^{p\mathbb{P}}(s') \tag{1.16}$$

where $f_{\mathbb{P}/p}(\xi, t)$ is called the *flux factor* of the pomeron and $\sigma_T^{p\mathbb{P}}(s')$ is the total cross section of the pomeron-proton scattering. The pomeron flux factor is defined as

$$f_{\mathbb{P}/p}(\xi, t) \equiv \frac{1}{16\pi}\beta_{\mathbb{P}}^{pp}(t)^2 \xi^{1-2\alpha_{\mathbb{P}}(t)} \tag{1.17}$$

$$\equiv \frac{1}{16\pi}\{\beta_{\mathbb{P}}^{pp}(0)F(t)\}^2 \xi^{1-2\alpha_{\mathbb{P}}(t)}, \tag{1.18}$$

where the t dependence of the $\beta_{\mathbb{P}}^{pp}$ is replaced by the proton form factor $F(t)$ probed with the pomeron. The form factor $F(t)$ cannot be determined by the Regge theory. A hypothesis that a pomeron mainly couples to the quark in the hadron like a photon can reproduce the data well [14]. This hypothesis results in that the $F(t)$ is proportional to the electromagnetic-like form factor,

$$F_1(t) = \frac{4m_p^2 - 2.8t}{4m_p^2 - t}\left(\frac{1}{1 - t/0.71}\right)^2 \tag{1.19}$$

where m_p is a mass of the proton. The flux factor using this hypothesis is called Donnachie-Landshoff flux and is expressed as,

$$f_{\mathbb{P}/p}(\xi, t) = \frac{9}{4\pi^2}\beta_0^2 F_1(t)^2 \xi^{1-2\alpha_{\mathbb{P}}(t)} \tag{1.20}$$

where β_0=3.202 GeV^{-2} is the effective pomeron-quark coupling.

1.3 Diffractive $b\bar{b}$ production

The factorization property of the pomeron is supported by the elastic and the diffractive scattering experiments and implies that a pomeron can be treated as an ordinary particle virtually emitted from a hadron. Ingelman and Schlein proposed to extend the formalism obtained in the soft diffraction into the region of the hard diffractive scattering [4]. According to their idea, we describe our model used to calculate the diffractive $b\bar{b}$ production cross section in the thesis. Assuming that the factorization property is kept in this scale, the cross section of the diffractive $b\bar{b}$ production can be expressed as,

$$\frac{d\sigma(p\bar{p} \to p + b\bar{b}X)}{dt\, d\xi\, dp_T^2} = f_{I\!P/p}(\xi, t) \frac{d\sigma(\bar{p}I\!P \to b\bar{b}X)}{dp_T{}^2}, \tag{1.21}$$

where,

$$\frac{d\sigma(\bar{p}I\!P \to b\bar{b}X)}{dp_T{}^2} = \sum_{i,j} \int dx_1 f_{a_i/\bar{p}}(x_1, p_T{}^2) \int dx_2 f_{b_j/I\!P}(x_2, p_T{}^2) \frac{d\sigma(a_i b_j \to b\bar{b}X')}{dp_T^2}, \tag{1.22}$$

and the p_T is the transverse momentum of the b-quarks. The $f_{a_i/\bar{p}}(x_1, p_T^2)$ and the $f_{b_j/I\!P}(x_2, p_T^2)$ are the structure function for anti-proton and pomeron, respectively. The sum is performed over all parton types. As stated in the previous section, the pomeron flux factor $f_{I\!P/p}(\xi, t)$ is not uniquely defined by the Regge phenomenology. We used the Donnachie-Landshoff flux (Eq.1.20) to calculate the theoretical prediction. (Ingelman and Schlein used a different flux parameterization in their original analysis [4].)

The pomeron structure function $f_{b_j/I\!P}(x_2, p_T^2)$ was recently measured by H1 [7] and ZEUS [8] using deep inelastic scattering processes. The extracted parton distribution turned out to be nearly flat. According to this result, we used a simple model for a pomeron structure function expressed as;

$$z f_{g,q/I\!P}(z) \sim 1. \tag{1.23}$$

Another frequently used structure function is a hard structure function,

$$z f_{g,q/I\!P}(z) \sim z(1-z) \tag{1.24}$$

which is derived from the assumption that two partons share the pomeron momentum. We also used the hard structure function in the analysis.

1.4 Outline of analysis procedure

One of the characteristic signature of the single diffraction is an absence of a beam jet in one side of the forward rapidity region where particles are usually observed in the non-diffractive $p\bar{p}$ collisions. This signature is owing to the color-less nature of the exchanged object and is called the forward *rapidity gap*. In order to tag the rapidity gap events, we used two forward detectors, the forward calorimeters and the BBC which partially overlap with each other. The rapidity gap signal in the single diffraction is sometimes killed because particles generated from the dissociating system give the signal in the detector. We have corrected this rate of inefficiency using results of the Monte Carlo study.

The b-quark production candidates are tagged using an electron in the central rapidity region. We select events with such an electron to make up an electron sample. The impact parameter distribution and the transverse momentum spectrum relative to the jet axis are used to estimate the $b\bar{b}$ event fraction in the electron sample. The diffractive b-quark production candidates are selected from the electron sample using the rapidity gap signal. The fraction of b-quark events are individually estimated for both diffractive and non-diffractive sample. After correcting the efficiency and acceptance for the rapidity gap tagging, the ratio of the diffractive to the non-diffractive b-quark production is measured. The results are finally compared to the theoretical prediction.